# Supporting Information

## Sea urchin-like amorphous MgNiCo mixed metal hydroxide nanoarrays for efficient overall water splitting at industrial electrolytic conditions

Liping Wang[§, a], Yikun Cheng[§, a], Jiahao Xiong[a], Zhiwen Zhao[a], Dingbo Zhang[a], Zhiyan Hu[a], Haoyu Zhang [a], Qin Wu [a], Long Chen*[, a]

[a] Key Laboratory for Green Process of Chemical Engineering of Xinjiang Bingtuan, School of Chemistry and Chemical Engineering, Shihezi University, Shihezi 832003, Xinjiang, China.

§ Co-authors

E-mail address: 1561538683@qq.com

E-mail address: 1754394006@qq.com

* Corresponding authors

E-mail address: chenlong2012@sinano.ac.cn (L. Chen).

# 1. Experimental Section

## 1.1. Material Characterization

The $Mg_xNi_{1-x}Co$-OH synthesized is reflected by X-ray powder diffractometry (XRD), wherein Cu Kα radiation (λ = 0.15406 nm) 2θ ranged from 20 to 80. The surface morphology and microstructure of nanocrystals $Mg_xNi_{1-x}Co$-OH and NiCo-OH are obtained by scanning electron microscopy (SEM; LEO1430VP, Germany) and transmission electron microscopy (TEM; FEI, Tecnai G2 F20 S-Twin, America).

## 1.2. Electrochemical Characterization

The electrochemical test of oxygen evolution reaction (OER) and hydrogen evolution reaction (HER) is performed at the CHI760e electrochemical workstation (CHI 760E, CH Instruments Inc., Shanghai, China). Using platinum wire, Ag/AgCl, and MgNiCo LDH/NF as the counter electrode, reference electrode, and working electrode, respectively. The reaction condition is at 1M KOH electrolyte 25℃. The overpotential is obtained by the formulation (1)(3) for OER and (1)(4) for HER. The LSV curves test for both HER and OER at the scan rate of 5mV/s. Hg/HgO makes the performance of the material better stable at the 5M KOH for HER and OER. So, we change to use carbon rod, Hg/HgO, and $Mg_xNi_{1-x}Co$-OH as the counter electrode, reference electrode, and working electrode, at the industrial electrolysis conditions (5M KOH 65℃). The overpotentials obtained for HER and OER are calculated according to formulation (2)(4)(3). Tafel Slope shows the reaction kinetics and catalytic activity of all catalysts. Calculated by the following formulation (5).

Turnover frequency (TOF) quantitative the OER activity, calculated by the following formulation (6)(7), respectively.

### 1.3. Calculation formulae

The reversible hydrogen electrode (RHE) potential for the HER and OER at 1M KOH 25℃ are calculated based on the test LSV curves [1, 2]:

$$E_{RHE} = E_{Ag/AgCl} + 0.197 + 0.059* PH \quad (1)$$

$$E_{RHE} = E_{Hg/HgO} + 0.095 + 0.059* PH \quad (2)$$

The overpotential (η) for HER and OER are calculated according to the following formulations [1]

$$\eta_{OER} = E_{RHE} - 1.23 \quad (3)$$

$$\eta_{HER} = E_{RHE} \quad (4)$$

The Tafel slope is obtained according to the following formulation [2], where η-Overpotential (mV), b-Tafel Slope, i-Current density (mA $cm^{-2}$).

$$\eta = a + b\log i \quad (5)$$

The computational formula for Turn over frequency (TOF) where j-current density (mA $cm^{-2}$). A -surface area (1 $m^2$) of NF with $Mg_{0.75}Ni_{0.25}$Co-OH, F -Faraday constant, and m-amounts of active sites in the catalysts [3].

$$TOF = \frac{j * A}{4 * F * m} \quad (6)$$

The mounts of active sites in the catalysts (m) are obtained by the following formulation, where n -the number of electrons transport (n=1), R-ideal gas constant, and T - absolute temperature, m is obtained by the following formulation.

$$slope = \frac{n^2 * F^2 * A * m}{4 * R * T} \quad (7)$$

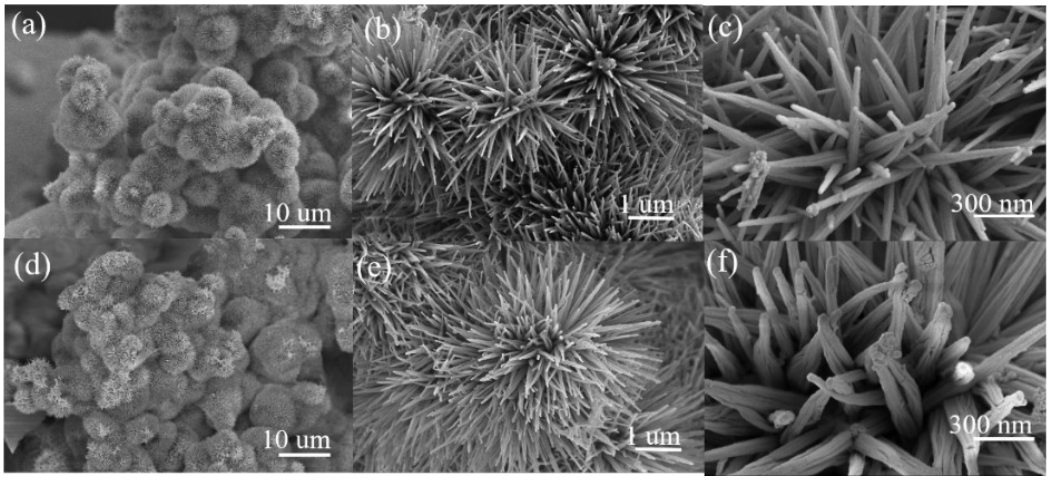


Fig. S1. SEM images of (a, b, c) $Mg_{0.25}Ni_{0.75}$Co-OH and (d, e, f) $Mg_{0.75}Ni_{0.25}$Co-OH.

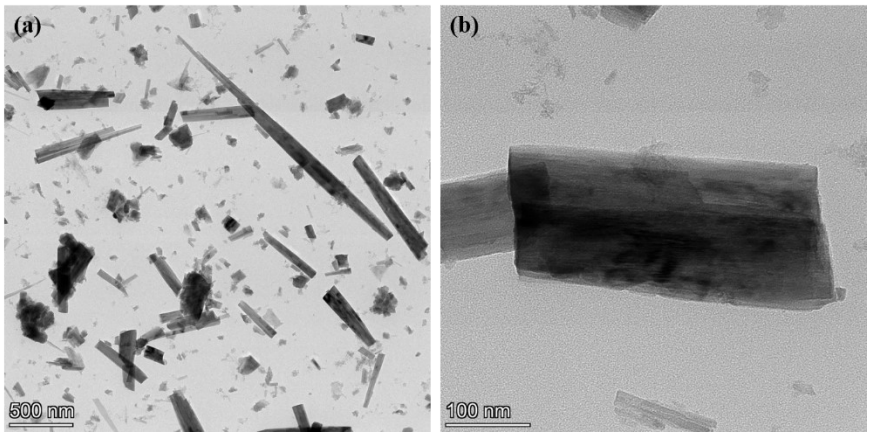


Fig. S2. TEM images of the $Mg_{0.5}Ni_{0.5}$Co-OH at high magnification(a) and low magnification

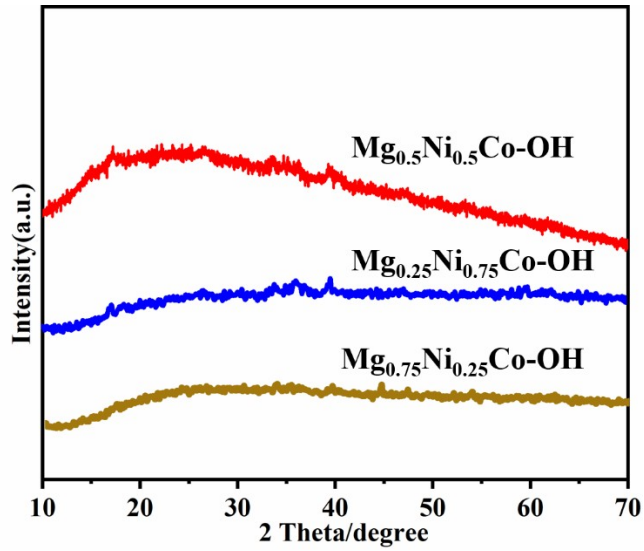


Fig. S3. XRD images of $Mg_{0.5}Ni_{0.5}$Co-OH, $Mg_{0.25}Ni_{0.75}$Co-OH and $Mg_{0.75}Ni_{0.25}$Co-OH

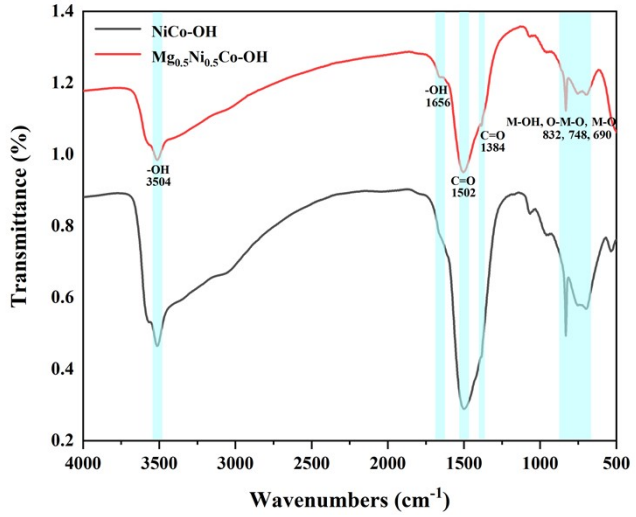


Fig. S4. FT-IR spectra of $Mg_{0.5}Ni_{0.5}$Co-OH and NiCo-OH

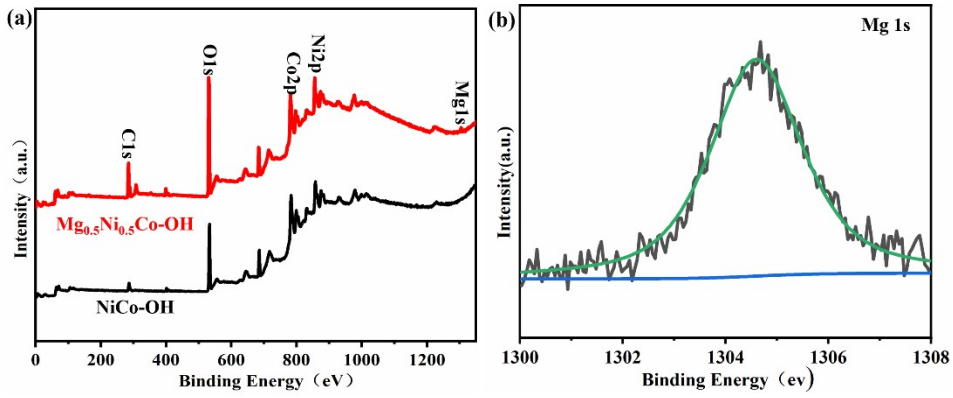

Fig. S5. (a) Survey XPS spectra of all samples. (b) XPS spectra of Mg1s.

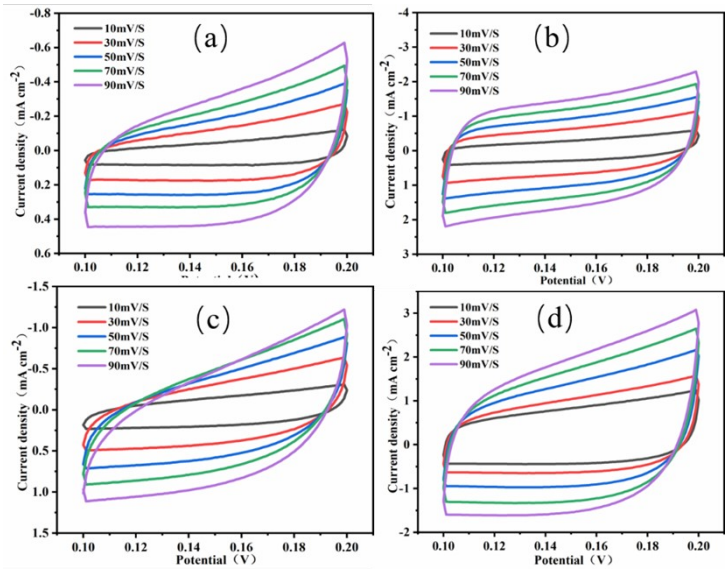


Fig. S6. CV curves measured with different scan rates of 10, 30, 50, 70, and 90 mV/s: (a) NiCo-OH, (b) $Mg_{0.5}Ni_{0.5}Co$-OH, (c) $Mg_{0.75}Ni_{0.25}Co$-OH, (d) $Mg_{0.25}Ni_{0.75}Co$-OH.

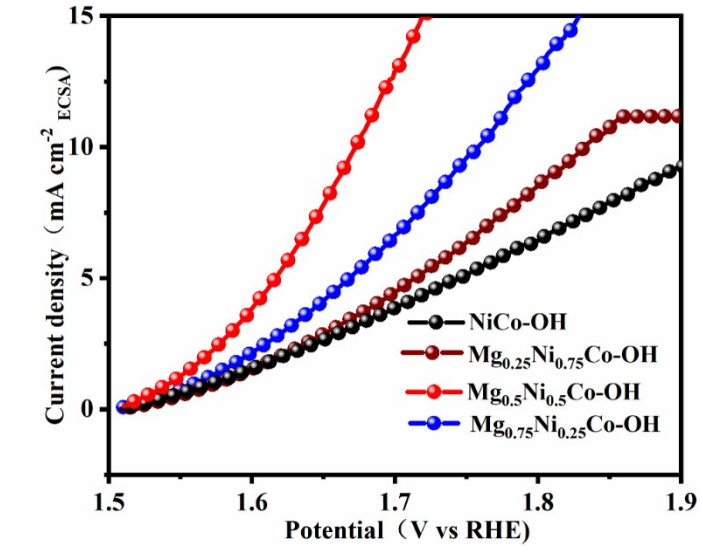


Fig. S7. (h) LSV curves normalized by ECSA of NiCo-OH, $Mg_{0.25}Ni_{0.75}Co$-OH, $Mg_{0.5}Ni_{0.5}Co$-OH, and $Mg_{0.75}Ni_{0.25}Co$-OH for OER.

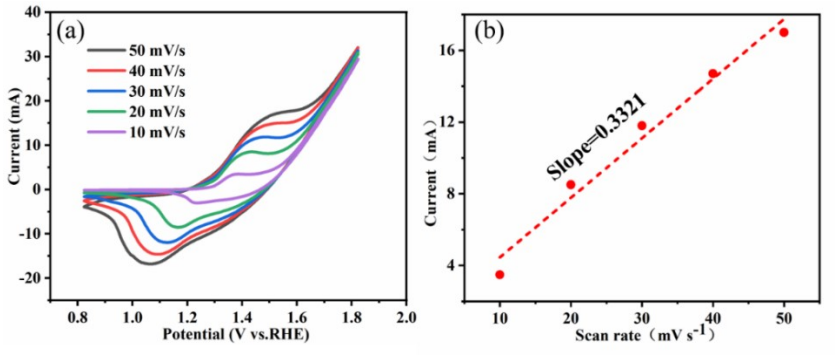


Fig. S8. (a) CV of $Mg_{0.5}Ni_{0.5}$Co-OH at different scan rates of 10, 20, 30, 40, and 50 mV $s^{-1}$ in 1 M KOH. (b) the relationship of the oxidation peak currents and scan rate.

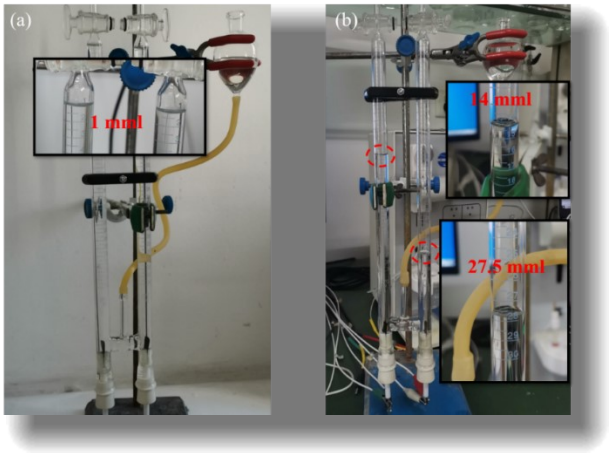


Fig. S9. A digital photograph of the Hoffman apparatus is used for the measurement of the Faradaic efficiency. (a) before test (b) after 320 min test at 12 mA $cm^{-2}$.

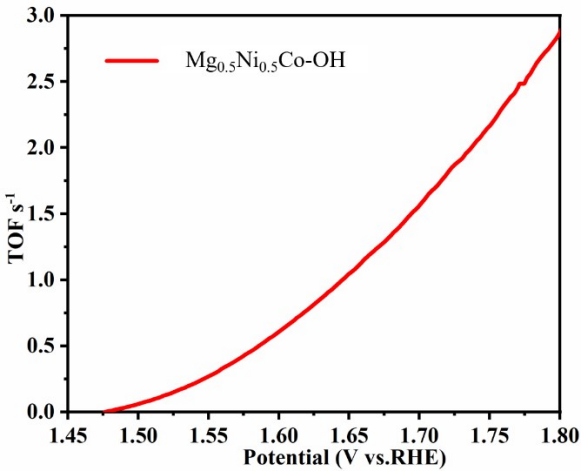


Fig. S10. The TOF curve of $Mg_{0.5}Ni_{0.5}Co$-OH

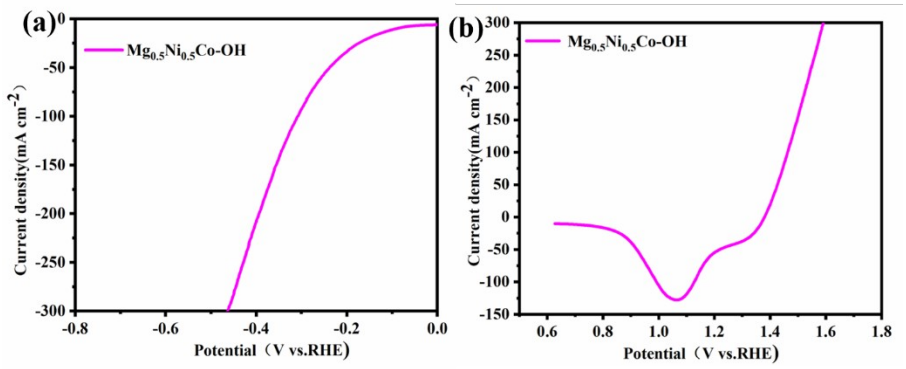


Fig. S11. LSV curve of $Mg_{0.5}Ni_{0.5}Co$-OH at 5M KOH 65℃ for (a) HER and (b) OER.

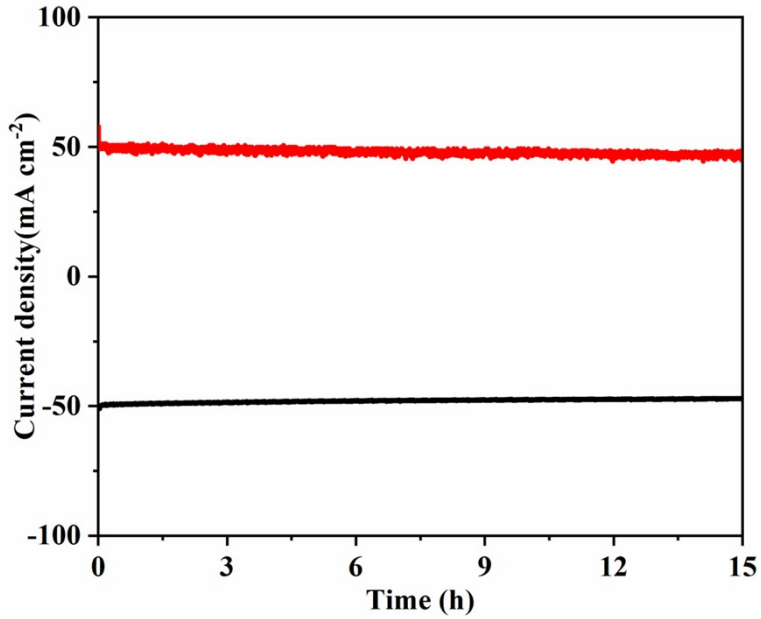


Fig. S12. The i-t curve of $Mg_{0.5}Ni_{0.5}Co$-OH at 5M KOH 65℃ for HER and OER.

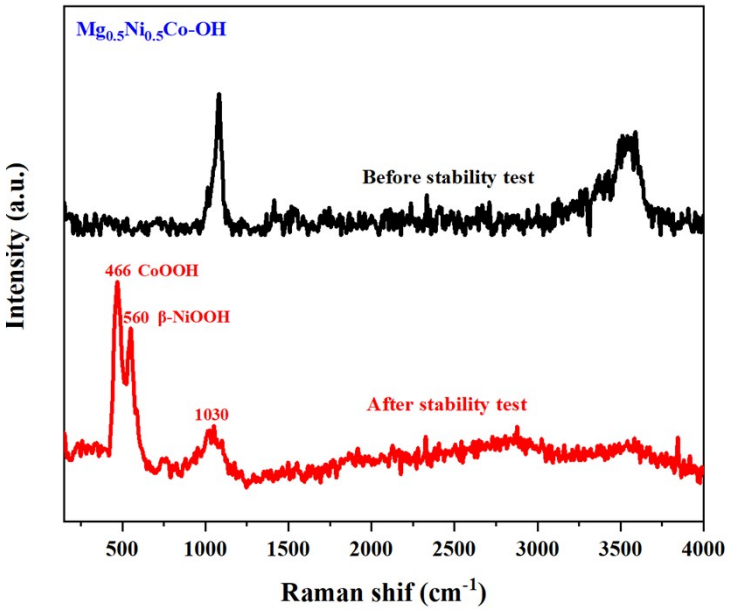


Fig. S13. Raman spectrum of $Mg_{0.5}Ni_{0.5}Co$-OH before and after stability test in 5M KOH 65℃.

Table S1 Atomic molar ratio of material feed and actual atomic molar ratio.

| Theoretical atomic ratio | | | Experimental atomic ratio | | |
|---|---|---|---|---|---|
| Sample | Element | Feeding molar Ratio(mmol) | Sample | Elements | Feeding molar Ratio(mmol) |
| NiCo-OH | Ni | 0.33 | NiCo-OH | Ni | 0.43 |
| | Co | 0.67 | | Co | 0.57 |
| $Mg_{0.25}Ni_{0.75}Co$-OH | Mg | 0.08 | $Mg_{0.25}Ni_{0.75}Co$-OH | Mg | 0.046 |
| | Ni | 0.26 | | Ni | 0.353 |
| | Co | 0.66 | | Co | 0.601 |
| $Mg_{0.5}Ni_{0.5}Co$-OH | Mg | 0.17 | $Mg_{0.5}Ni_{0.5}Co$-OH | Mg | 0.05 |
| | Ni | 0.17 | | Ni | 0.347 |
| | Co | 0.67 | | Co | 0.604 |
| $Mg_{0.75}Ni_{0.25}Co$-OH | Mg | 0.25 | $Mg_{0.75}Ni_{0.25}Co$-OH | Mg | 0.165 |
| | Ni | 0.08 | | Ni | 0.252 |
| | Co | 0.67 | | Co | 0.582 |

Table S2 the impedance value for different samples of HER

| Electrocatalysts | Rs (Ω) |
|---|---|
| NiCo-OH | 5.53 Ω |
| $Mg_{0.25}Ni_{0.75}Co$-OH | 4.872 Ω |
| $Mg_{0.5}Ni_{0.5}Co$-OH | 3.337 Ω |
| $Mg_{0.75}Ni_{0.25}Co$-OH | 3.684 Ω |

Table S3 Performance of electrocatalysts for HER in 1M KOH

| Catalysts | Current density (mA $cm^{-2}$) | Potential (mV) (@10 mA $cm^{-2}$) | references |
|---|---|---|---|
| $Mg_{0.5}Ni_{0.5}Co$-OH | 10 | 110 | This work |
| V-NiFe LDH/NF | 10 | 120 | [4] |
| NiFe LDH/$(NiFe)S_x$ | 10 | 157 | [5] |
| LDH-$Co_3O_4$/NF | 10 | 162 | [6] |
| Cu@CoFe LDH | 10 | 171 | [7] |
| CoFe LDH-F | 10 | 166 | [8] |
| $NiCo_2S_4$@NiFe LDH | 10 | 200 | [9] |
| Co-N-C-800 | 10 | 224 | [10] |
| $CoCo_3$@NiFe LDH | 10 | 171 | [11] |

Table S4 the impedance value for different samples for OER

| Electrocatalysts | Rs (Ω) |
|---|---|
| NiCo-OH | 1.672 |
| $Mg_{0.25}Ni_{0.75}Co$-OH | 1.57 |
| $Mg_{0.5}Ni_{0.5}Co$-OH | 1.304 |
| $Mg_{0.75}Ni_{0.25}Co$-OH | 1.403 |

Table S5 Performance of electrocatalysts for OER

| catalysts | Current density ($mA\ cm^{-2}$) | Overpotential (mV) (@10 $mA\ cm^{-2}$) | references |
|---|---|---|---|
| $Mg_{0.5}Ni_{0.5}Co$-OH | 10 | 277 | This work |
| $HCo_3O_4$-NC@CoNi LDH | 10 | 330 | [12] |
| Co-B | 10 | 320 | [13] |
| (Co, Ni)$Se_2$@NiFe LDH | 10 | 277 | [14] |
| NiFe LDH@Co, N-CNF | 10 | 312 | [15] |
| Co-NiMn LDH | 10 | 310 | [16] |
| Co-LDH@$Ti_3C_2T_X$ | 10 | 340 | [17] |
| Fe-doped $Co_4S_3/Co_9S_8$ | 10 | 354 | [18] |
| $NiCo_2O_4$-MCNTs | 10 | 350 | [19] |

Table S6 Comparison of overpotentials of selected electrocatalysts to deliver 10 mA cm-2 for water splitting in 1.0 M KOH.

| Catalysts | Current density ($mA\ cm^{-2}$) | Potential (V) | References |
|---|---|---|---|
| $Mg_{0.5}Ni_{0.5}Co$-OH | 10 | 1.617 | This work |
| NF@G-5@$Ni_3S_2$ | 10 | 1.62 | [20] |
| $Ni_{0.85}Se$/RGO | 10 | 1.64 | [21] |
| Ni-Mo-S@CC (1:3) | 10 | 1.66 | [22] |
| Ni(II, III)Zn-LDH/NF-nm | 10 | 1.68 | [23] |
| $Co_{1.4}Ni_{0.6}O_2$ | 10 | 1.75 | [24] |
| NCP@WPCA-0.5 | 10 | 1.76 | [25] |
| $Ni_2P$/rGO/NF | 10 | 1.676 | [26] |

## References

1 H. Li, L. Chen, P. Jin, H. Lv, H. Fu, C. Fan and Y. Shi, Synthesis of $Co_{2-x}Ni_xO_2$ ($0 < x < 1.0$) hexagonal nanostructures as efficient bifunctional electrocatalysts for overall water splitting. Dalton Trans., 2020, 49, 6587-6595.

2 B. J. Rani, G. Ravi, R. Yuvakkumar, S. I. Hong, D. Velauthapillai, M. Thambidurai, C. Dang, B. Saravanakumar, Neutral and alkaline chemical environment dependent synthesis of $Mn_3O_4$ for oxygen evolution reaction (OER). Mater. Chem. Phys., 2020, 247, 122864.

3 J. Han, J. Zhang, T. Wang, Q. Xiong, W. Wang, L. Cao and B. Dong, Zn Doped FeCo Layered Double Hydroxide Nanoneedle Arrays with Partial Amorphous Phase for Efficient Oxygen Evolution Reaction. ACS Sustain. Chem. Eng., 2019, 7, 13105-13114.

4 J. Liang, H. Shen, Y. Ma, D. Liu, M. Li, J. Kong, Y. Tang and S. Ding, Autogenous growth of the hierarchical V-doped NiFe layer double metal hydroxide electrodes for an enhanced overall water splitting. Dalton Trans., 2020, 49, 11217-11225.

5 Y. Zou , B. Xiao , J. Shi , H. Hao , D. Ma , Y. Lv , G. Sun , J. Li and Y. Cheng, 3D hierarchical heterostructure assembled by NiFe LDH/$(NiFe)S_x$ on biomass-derived hollow carbon microtubes as bifunctional electrocatalysts for overall water splitting. Electrochim. Acta, 2020, 348, 136339.

6 J. Wang and Y. Song, Synchronous Electrocatalytic Design of Architectural and Electronic Structure Based on Bifunctional LDH-$Co_3O_4$/NF toward Water Splitting. Chem. Eur. J., 2021, 27, 3367-3373.

7 L. Yu , H. Zhou , J. Sun , F. Qin , D. Luo , L. Xie , F. Yu , J. Bao , Y. Li , Y. Yu , S.

Chen and Z. Ren, Hierarchical Cu@CoFe layered double hydroxide core-shell nanoarchitectures as bifunctional electrocatalysts for efficient overall water splitting. Nano Energy, 2017, 41, 327-336.

8 P. Liu, S. Yang, B. Zhang and H. Yang, Defect-Rich Ultrathin Cobalt–Iron Layered Double Hydroxide for Electrochemical Overall Water Splitting. ACS Appl. Mater. Interfaces, 2016, 8, 34474-34481.

9 J. Liu, J. Wang, B. Zhang, Y. Ruan, L. Lv, X. Ji, K. Xu and L. Miao, Jianjun Jiang Hierarchical $NiCo_2S_4$@NiFe LDH Heterostructures Supported on Nickel Foam for Enhanced Overall-Water-Splitting Activity. ACS Appl. Mater. Interfaces, 2017, 9, 15364-15372.

10 X. Chen, X. Zhen, H. Gong, L. Li, J. Xiao, Z. Xu, D. Yan, G. Xiao and R. Yang, Cobalt and nitrogen codoped porous carbon as superior bifunctional electrocatalyst for oxygen reduction and hydrogen evolution reaction in alkaline medium. Chin Chem Lett, 2019, 30, 681-685.

11 R. Que, S. Liu, P. He, Y. Yang and Y. Pan, Hierarchical heterostructure $CoCO_3$@NiFe LDH nanowires array as outstanding bifunctional electrocatalysts for overall water splitting. Mater. Lett., 2020, 277, 128285.

12 H. Zhang, Y. Tong, J. Xu, Q. Lu and F. Gao, In Situ Antisolvent Approach to Hydrangea-like $HCo_3O_4$-NC@CoNi-LDH Core@Shell Superstructures for Highly Efficient Water Electrolysis. Chemistry, 2018, 24, 400-408.

13 Y. Li, H. Xu, H. Huang, L. Gao, Y. Zhao and T. Ma, Synthesis of Co-B in porous carbon using a metal-organic framework (MOF) precursor: A highly efficient catalyst

for the oxygen evolution reaction. Electrochem commun, 2018, 86, 140-144.

14 J. Li, H. Sun, L. Lv, Z. Li, X Ao, C. Xu, Y. Li and C. Wang, Metal-Organic Framework-Derived Hierarchical (Co, Ni) $Se_2$@NiFe LDH Hollow Nanocages for Enhanced Oxygen Evolution. ACS Appl. Mater. Interfaces, 2019, 11, 8106-8114.

15 Q. Wang, L. Shang, R. Shi, X. Zhang, Y. Zhao, G. I. N. Waterhouse, L. Wu, C. H. Tung and T. Zhang, Zinc-Air Batteries: NiFe Layered Double Hydroxide Nanoparticles on Co, N-Codoped Carbon Nanoframes as Efficient Bifunctional Catalysts for Rechargeable Zinc-Air Batteries. Adv. Energy Mater., 2017, 7, 1700467.

16 Y. Wang, X. Liu, N. Zhang, G. Qiu and R. Ma, Cobalt-doped Ni-Mn layered double hydroxide nanoplates as high-performance electrocatalyst for oxygen evolution reaction. Appl Clay Sci, 2018, 165, 277-283.

17 M. Benchakar, T. Bilyk, C. Garnero, L. Loupias, C. Morais, J. Pacaud, C. Canaff, P. Chartier, S. Morisset, N. Guignard, V. Mauchamp, S. Célérier and A. Habrioux, MXene Supported Cobalt Layered Double Hydroxide Nanocrystals: Facile Synthesis Route for a Synergistic Oxygen Evolution Reaction Electrocatalyst. Adv. Mater. Interfaces., 2019, 6, 1901328.

18 F. Chen, Z. Zhang, W. Liang, X. Qin, Z. Zhang and L. Jiang, Synthesis of $Co_4S_3$/$Co_9S_8$ nanosheets and comparison study toward the OER properties induced by different metal ion doping. Chin Chem Lett, 2022, 33, 1395-1402.

19 E. Umeshbabu, P. H. K. Charan, P. Justin and G. R. Rao, Hierarchically Organized $NiCo_2O_4$ Microflowers Anchored on Multiwalled Carbon Nanotubes: Efficient Bifunctional Electrocatalysts for Oxygen and Hydrogen Evolution Reactions.

ChemPlusChem, 2020, 85, 183-194.

20 C. Jin, N. Zhou, Y. Wang, X. Li, M. Chen, Y. Dong, Z. Yu, Y. Liang, D. Qu, Y. Dong, Z. Xie and C. Zhang, 3D porous and self-supporting Ni foam@graphene@$Ni_3S_2$ as a bifunctional electrocatalyst for overall water splitting in alkaline solution. J. Electroanal. Chem., 2020, 858, 113795.

21 G. Liu, C. Shuai, Z. Mo, R. Guo, N. Liu, X. Niu, Q. Dong, J. Wang, Q. Gao, Y. Chen and W. Liu, One-pot synthesis porous nanosphere $Ni_{0.85}Se$ on graphene as efficient and durable electrocatalyst for overall water splitting. New J. Chem., 2020, 44, 17313-17322.

22 Y. Wang, W. Sun, X. Ling, X. Shi, L. Li, Y. Deng, C. An and X. Han, Bimetallic phosphide nanoparticles embedded in carbon nanostrips for electrocatalytic water oxidation. Chem. Eur. J., 2020, 26, 4097-4103.

23 Y. Gong, J. Huang, L. Cao, K. Kajiyoshi, D. Yang, Y. Feng, L. Kou and L. Feng, Methanol-assisted synthesis of $Ni^{3+}$ - doped ultrathin NiZn-LDH nanomeshes for boosted alkaline water splitting. Dalton Trans., 2020, 49, 1325-1333.

24 H. Li, L. Chen, P. Jin, H. Lv, H. Fu, C. Fan, S. Peng, G. Wang, J. Hou, F. Yu and Y. Shi, Synthesis of $Co_{2-x}Ni_xO_2$ ($0<x<1.0$) hexagonal nanostructures as efficient bifunctional electrocatalysts for overall water splitting. Dalton Trans., 2020, 49, 6587-6595.

25 C. Wang, L. Kong, H. Sun, M. Zhong, H. Cui, Y. Zhang, D. Wang, J. Zhu and X. Bu, Carbon Layer Coated $Ni_3S_2/MoS_2$ Nanohybrids as Efficient Bifunctional Electrocatalysts for Overall Water Splitting. ChemElectroChem, 2019, 6, 5603-5609.

26 J. Huang, F. Li, B. Liu and P. Zhang, $Ni_2P$/rGO/NF Nanosheets As a Bifunctional High-Performance Electrocatalyst for Water Splitting. Materials, 2020, 13, 744.